The EMBO Journal Vol.17 No.16 pp.4798–4808, 1998

Cooperative modulation by eIF4G of eIF4E-binding to the mRNA 5′ cap in yeast involves a site partially shared by p20

Marina Ptushkina, Tobias von der Haar, Simona Vasilescu, Ronald Frank[1], Ralf Birkenhäger and John E.G.McCarthy[2]

Posttranscriptional Control Group, Department of Biomolecular Sciences, UMIST, P.O. Box 88, Manchester M60 1QD, UK and [1]Molecular Recognition Research Group, Gesellschaft für Biotechnologische Forschung mbH, Mascheroder Weg 1, D-38124 Braunschweig, Germany

[2]Corresponding author
e-mail: J.McCarthy@umist.ac.uk

T.von der Haar and M.Ptushkina contributed equally to this work

Interaction between the mRNA 5′-cap-binding protein eIF4E and the multiadaptor protein eIF4G has been demonstrated in all eukaryotic translation assemblies examined so far. This study uses immunological, genetic and biochemical methods to map the surface amino acids on eIF4E that contribute to eIF4G binding. Cap-analogue chromatography and surface plasmon resonance (SPR) analyses demonstrate that one class of mutations in these surface regions disrupts eIF4E–eIF4G association, and thereby polysome formation and growth. The residues at these positions in wild-type eIF4E mediate positive cooperativity between the binding of eIF4G to eIF4E and the latter's cap-affinity. Moreover, two of the mutations confer temperature sensitivity in eIF4G binding to eIF4E which correlates with the formation of large numbers of inactive ribosome 80S couples *in vivo* and the loss of cellular protein synthesis activity. The yeast 4E-binding protein p20 is estimated by SPR to have a ten times lower binding affinity than eIF4G for eIF4E. Investigation of a second class of eIF4E mutations reveals that p20 shares only part of eIF4G's binding site on the cap-binding protein. The results presented provide a basis for understanding how cycling of eIF4E and eIF4G occurs in yeast translation and explains how p20 can act as a fine, but not as a coarse, regulator of protein synthesis.

Keywords: cooperativity/eIF4E and eIF4G/interaction sites/regulation by 4E-binding proteins/yeast gene expression

Introduction

The eukaryotic initiation factor 4E (eIF4E) is an essential protein that anchors the mRNA cap-binding complex (eIF4F) to the 5′ end of capped mRNAs (Sonenberg, 1996). The eIF4F complex, which plays a key role in the mediation of interactions between the 40S ribosomal subunit and mRNA, varies in composition from organism to organism. In the mammalian complex, eIF4E is associated with two other factors, eIF4G and eIF4A. This association is mediated via binding sites for eIF4E and eIF4A on eIF4G, and the additional presence of an eIF3 binding site on eIF4G is also thought to allow the tethering of mRNA-bound eIF4F to the 40S ribosomal subunit (Lamphear *et al.*, 1995; Merrick and Hershey, 1996), thus promoting the first phase of translational initiation. The inclusion of eIF4A in the eIF4F complex is significant because eIF4A, together with eIF4B, exhibits ATP-dependent bidirectional RNA helicase activity that is potentially capable of unwinding structured mRNA (Rozen *et al.*, 1990). In contrast, neither the yeast (Lanker *et al.*, 1992; Ptushkina *et al.*, 1996) nor the plant (Browning, 1996) eIF4F complexes that have been analysed show a strong association with eIF4A. However, all types of eIF4F investigated so far include eIF4E and one or other version of the eIF4G factor, and this core complex is therefore a common and essential feature of eukaryotic translational initiation. In the budding yeast *Saccharomyces cerevisiae*, two similar versions of eIF4G (1 and 2; otherwise known as p150 and p130; Goyer *et al.*, 1993) can bind to eIF4E. Apart from carrying a binding site for eIF4E, *S.cerevisiae* eIF4G also has a site of interaction with the poly(A) binding protein (Pab1p) which has been localized by means of deletion analysis to the N-terminal region (Tarun and Sachs, 1996). The interaction with Pab1p is not essential for cell viability (Tarun *et al.*, 1997) while this property is apparently shared by wheat eIF-iso4G (Le *et al.*, 1997) but not by human eIF4GI/II or *Schizosaccharomyces pombe* eIF4G (Morley *et al.*, 1997; Gradi *et al.*, 1998; M.Ptushkina and J.E.G.McCarthy, unpublished data). On the other hand, a very recent report describes a 480 amino acid human PABP-binding protein that shows similarity to the central region of eIF4G (Craig *et al.*, 1998).

In contrast, all of the full-length eIF4G proteins examined up to now contain an N-terminal binding site for eIF4E (Lamphear *et al.*, 1995; Mader *et al.*, 1995; Browning, 1996; Morley *et al.*, 1997; McCarthy, 1998). This binding site includes a 10 amino acid motif which features a generally conserved pattern of charged, aliphatic and aromatic side chains (Altmann *et al.*, 1997). Mutations in this motif reduce eIF4G–eIF4E affinity in the mammalian system (Mader *et al.*, 1995), and can generate a temperature-sensitive phenotype in *S.cerevisiae* (Tarun *et al.*, 1997). Natural regulatory proteins in mammalian cells, called 4E-binding proteins (4E-BPs), have a related motif (Pause *et al.*, 1994). The binding of the 4E-BPs to eIF4E (via interactions involving this motif) can block formation of eIF4E–eIF4G, and is regulated via the state of phosphorylation of these regulatory proteins (Pause *et al.*, 1994). *Saccharomyces cerevisiae* currently has only one potential candidate for this role, called p20 (Lanker *et al.*, 1992; Altmann *et al.*, 1997), which has a molecular weight of ~18 kDa (Zanchin and McCarthy, 1995). Like the mammalian 4E-BPs, p20 shows variable phosphorylation states (Zanchin and McCarthy, 1995). Moreover, a p20–

glutathione *S*-transferase (GST) fusion protein was found to compete with eIF4G for binding to eIF4E (Altmann *et al.*, 1997). Thus work so far has suggested that p20 may constitute a regulatable equivalent to a mammalian 4E-BP in yeast.

While much attention to date has been focused on the interaction sites of eIF4G, almost nothing is known about the protein-binding sites on eIF4E and the functional influence of interactions at these sites. In the present work we use biochemical, immunological and genetic methods to study the molecular basis of specific eIF4G binding by eIF4E in yeast. We find that this specific interaction is strong (estimated K_d = 10^{-8}–10^{-9} l/mol at 25°C) and involves a combination of surface residues on yeast eIF4E that are highly conserved among all the known eIF4E proteins. The eIF4G–eIF4E interaction enhances eIF4E cap-binding activity, thus providing the molecular basis for a potential loading–release cycle for eIF4F and mRNA. In contrast, we find that p20 shares only part of the eIF4G binding site, and its affinity for eIF4E is estimated to be lower than that of eIF4G. Moreover, p20 binding has a less pronounced effect on the eIF4E–cap interaction. These newly characterized properties of eIF4E interactions with the cap, the eIF4E-binding domain of eIF4G, and p20 provide a quantitative basis for a model of eIF4E function and regulation.

Results

Heterotropic cooperativity of binding sites on eIF4E

Yeast eIF4E can interact with either eIF4G or p20 as well as the 5′ cap of mRNA. In the first stage of our investigation of these interactions, we examined whether there is cooperativity between the respective binding sites. Recent work has shown that the cross-linking signal obtained with human eIF4E and the 5′ cap structure is enhanced in the presence of eIF4G (Haghighat and Sonenberg, 1997), thus providing indirect evidence of a change in cap affinity. Our initial objective was to determine whether the cap-binding affinity of yeast eIF4E is subject to modulation by virtue of its interactions with binding sites on eIF4G or p20, and if so, whether this modulation is negative or positive. In order to perform these experiments, we generated eIF4E, p20 and the eIF4E-binding domain of eIF4G1 in *Escherichia coli* using expression vectors carrying all or part of the corresponding yeast genes (*CDC33*, *CAF20* and *TIF4631*, respectively). Six-histidine (His_6) tags were added to the latter binding domain and to p20 (4G-BD4E$_{His6}$ and p20$_{His6}$; Figure 1B). Alternatively, a FLAG-tag was added to the C-terminal end of 4G-BD4E (Figure 1A). The ability of 4G-BD4E to bind yeast eIF4E under normal cellular conditions was confirmed by expressing the FLAG-tagged version of this construct in a yeast wild-type strain and preparing extracts for the analysis of cap-binding proteins (Figure 1A). Because of the marked protease sensitivity of p20, we found that stable, homogeneous preparations of p20$_{His6}$ were only obtainable with the help of a protease-reduced strain of *E.coli* (strain CAG629; Grossman *et al.*, 1984).

We investigated whether the cap-binding affinity of eIF4E can be modulated by interactions with the other two protein ligands. eIF4E bound to m^{7}GDP–Sepharose

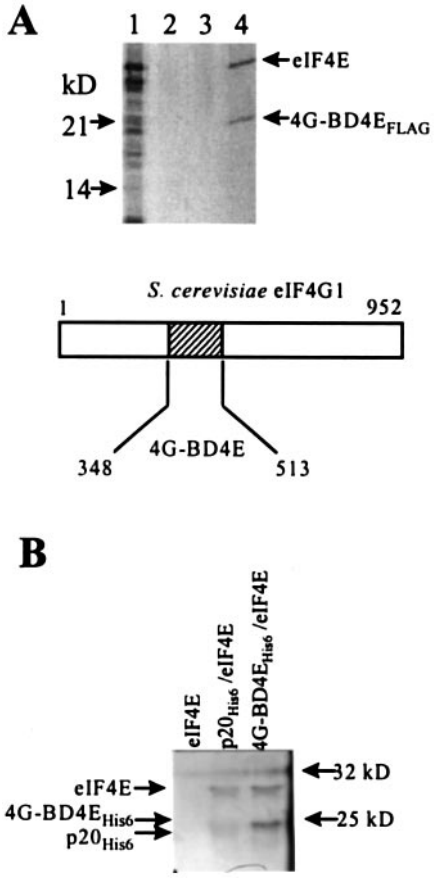

Fig. 1. The influence of eIF4E interactions with the eIF4E-binding domain of eIF4G and with p20 on cap binding. The eIF4E-binding domain subcloned from *S.cerevisiae* TIF4631 bound to eIF4E in the cap-binding fraction isolated from a yeast strain carrying the 4G-BD4E$_{FLAG}$ expression construct. (**A**) Cell extracts were passed over an m^{7}GDP–Sepharose column and the following fractions collected for SDS–PAGE and silver-staining: lane 1, the run-through fraction; lane 2, the buffer A wash; lane 3, the GDP-wash; lane 4, elution with m^{7}GDP (see Materials and methods). 4G-BD4E$_{FLAG}$ emerged associated with eIF4E in the m^{7}GDP elution fractions. The 4G-BD4E domain was also synthesized as a C-terminally tagged poly(His) version in *E.coli* and purified for use in binding experiments with recombinant eIF4E *in vitro*. (**B**) eIF4E was first allowed to bind to m^{7}GDP–Sepharose, after which the eIF4E associated with the column material was incubated with 4G-BD4E$_{His6}$, p20$_{His6}$ or with buffer alone. Finally, after elution with m^{7}GDP the elution fractions were subjected to SDS–PAGE. The eIF4E band in the experiment lacking a protein ligand (lane 'eIF4E') is so weak as to be barely visible in this reproduction. p20 is stained poorly by silver, and therefore appears as a relatively weak band. In both types of experiment [(A) and (B)], the positions of protein molecular weight standards and of specific proteins are indicated on the sides of the gels.

was exposed to a fixed quantity of buffer containing no eIF4E, and the system was allowed to adjust to a new equilibrium state of bound and unbound eIF4E (Figure 1B). Addition of a molar equivalent amount of 4G-BD4E$_{His6}$ was found to reduce greatly the amount of eIF4E released from the cap-analogue affinity material, thus demonstrating that the cap-binding affinity of the 4G-BD4E$_{His6}$–eIF4E complex is much enhanced relative to that of eIF4E alone (Figure 1B). A weaker positive cooperative binding effect was observed upon introduction of p20$_{His6}$ into the incubation medium. Thus, while the binding of eIF4G and p20

to eIF4E are mutually exclusive, the functional effects of binding of these two proteins on eIF4E–cap interactions are not identical. We next set out to investigate the binding sites on eIF4E and the characteristics of the interactions in more detail.

Mapping of interaction sites using monoclonal antibodies

Given the general lack of information about the roles of surface residues on eIF4E, we initiated our search for amino acids involved in binding by generating a random set of monoclonal antibodies directed against active recombinant *S.cerevisiae* eIF4E purified from *E.coli.* The epitopes of the monoclonal antibody preparations were mapped using overlapping dodecameric and decameric synthetic peptides covalently attached to paper filters (Figure 2A). Analysis of binding data revealed the existence of epitopes distributed over much of the peptide chain (Figure 2B). None of the monoclonal antibodies screened were found to be specific for epitopes in the region 105–165. This was assumed to be due to the low accessibility and/or poor antigenicity of amino acids in this region. Since we also found that monoclonal antibodies directed against *S.pombe* eIF4E did not manifest epitope specificities in the equivalent region, we conclude that this is attributable to natural features common to eIF4E proteins. Indeed, the recently published crystal structure of an N-terminally truncated form of mouse eIF4E indicates that 65% of the side chains in the region 110–170 are not solvent accessible (Marcotrigiano *et al.*, 1997). In the subsequent analysis of interactions between the monoclonal antibodies and eIF4E, we excluded those recognizing the extreme N-terminal and C-terminal epitopes (2E9, 6D10, 1–2, 6H11 and 4H12) because earlier work had shown that the regions covered could be deleted without eliminating eIF4E function *in vivo* (Vasilescu *et al.*, 1996).

The monoclonal antibodies were then used in the coarse mapping of functional sites on eIF4E. Two types of interaction were investigated: binding to 4G-BD4E$_{His6}$ and cap recognition. Analysis of the effects of the monoclonal antibodies on eIF4E–4G-BD4E$_{His6}$-binding involved preincubation of the two yeast proteins with the antibodies followed by affinity chromatography on a m^{7}GDP–Sepharose column. The respective complexes were eluted from the affinity column and analysed by means of SDS–polyacrylamide electrophoresis (SDS–PAGE) followed by silver-staining (Figure 3). Four of the monoclonal antibodies (5C1, 6C1, 1D10 and 4E10) were capable of competing with eIF4E–4G-BD4E$_{His6}$ interactions, whereby the effect of 1D10 was very weak. This competition effect was evident from the fact that the relative amount of 4G-BD4E$_{His6}$ coeluting with eIF4E from the m^{7}GDP–Sepharose material was decreased. The observation that the effectiveness of the respective monoclonal antibodies as competitors varied is expected, since the binding affinities of individual monoclonal antibodies for their respective epitopes can vary over a considerable range (K_d = 10^{-5}–10^{-12} l/mol; Harlow and Lane, 1988). A different subset of the monoclonal antibodies (5C1 and 1F2) inhibited directly the binding of eIF4E (in the absence of 4G-BD4E$_{His6}$) to the m^{7}GDP column (data not shown). This was also reflected in the particularly poor yield

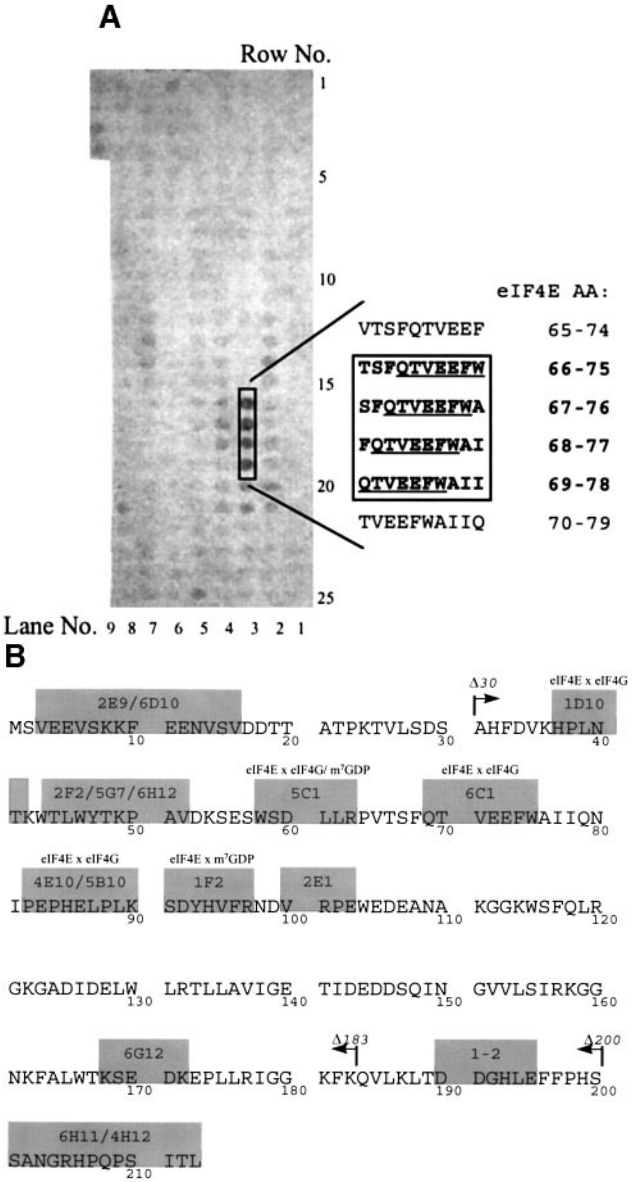

Fig. 2. Epitope-mapping of monoclonal antibodies directed against *S.cerevisiae* eIF4E. The example shown in (**A**) represents the fine mapping with decameric peptides for the anti-eIF4E monoclonal antibody 6C1. The identities of the respective peptides bound at the positive positions are indicated in the box to the right of the peptide matrix. The sequence common to all four of the clearly positive spots is underlined. This corresponds to the region 69–75 in the amino acid sequence of *S.cerevisiae* eIF4E [compare with (**B**)]. The epitopes determined in this way for the set of monoclonal antibodies are indicated by grey boxes in (B).

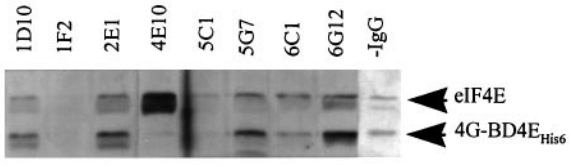

Fig. 3. Specific anti-eIF4E monoclonal antibodies inhibit eIF4E binding to the eIF4E-binding domain of eIF4G and/or to m^{7}GDP–Sepharose. The respective antibodies (as indicated above the gel) were preincubated with eIF4E and 4G-BD4E$_{His6}$, and the incubation mixtures were then subjected to affinity chromatography using m^{7}GDP–Sepharose. The fractions eluted using m^{7}GDP were then subjected to SDS–PAGE and silver-staining.

of eIF4E observed in the eIF4E–4G-BD4E$_{His6}$ complex binding experiments (Figure 3).

A further aspect of these data was that in two cases where the monoclonal antibody competed only with 4G-BD4E$_{His6}$ for binding to eIF4E and had been shown not to affect eIF4E cap affinity directly (6C1 and 1D10), the total amount of eIF4E bound to the affinity column was also reduced. This was consistent with the observation that the wild-type eIF4E–4G-BD4E$_{His6}$ interaction increases the cap-binding affinity of eIF4E, so that interfering with the interaction might be expected to result in poor cap binding. However, the binding of 4E10 produced a different response: in this case the antibody blocked eIF4G binding while apparently forcing eIF4E to assume its high cap-binding-affinity form (Figure 3). This is also fully consistent with the operation of cooperative enhancement of cap binding, since 4E10 seems to bind a site that locks eIF4E into the enhanced affinity conformation. Further evidence of the relationship between eIF4E–eIF4G interactions and enhanced cap binding by eIF4E was obtained from the mutational analysis described in the following section.

The above experiments generated an initial low resolution map relating epitope binding to specific functions (Figure 2B). Comparison of these monoclonal antibody competition data with the crystal structure of an N-terminally shortened mouse eIF4E (Marcotrigiano *et al.*, 1997) and the nuclear magnetic resonance (NMR) structure for yeast eIF4E embedded in CHAPS micelles (Matsuo *et al.*, 1997) provides a useful guide to areas that could be directly relevant to eIF4E binding activities. The epitopes we have found to influence eIF4E binding to the cap or to eIF4G include amino acids identified in the solved structures of eIF4E as being surface residues (a number of residues in the region 58–90; compare with Matsuo *et al.*, 1997).

Moreover, consistent with their inhibitory influence on cap binding, the monoclonal antibodies 5C1 and 1F2 recognize epitopes that include (i.e. W58 and L62 in the epitope 5C1) or are close to (W104 adjacent to the epitope 1F2) residues predicted on the basis of the solved structures to participate in cap interactions.

Highly conserved surface residues are involved in eIF4E–eIF4G interactions

The results of the monoclonal antibody studies indicated that highly conserved residues in the region 58–90 of the eIF4E protein sequence are involved in eIF4G binding. The structural studies of mouse and yeast eIF4E (Marcotrigiano *et al.*, 1997; Matsuo *et al.*, 1997) did not characterize the binding site for eIF4G. However, referring to the crystal structure of mouse eIF4E (Marcotrigiano *et al.*, 1997), we noted that the region 69–73 of helix 1 contains three surface residues that are highly conserved among the known eIF4E sequences (equivalent to residues 71–75 in the *S.cerevisiae* sequence; Figure 4). Moreover, the crystal structure indicates that this region lies close to a further group of outwardly oriented amino acids in helix 2 of the mouse protein that are also highly conserved (L131, G139, E140 and D143; Figure 4). The 71–75 and 131–143 regions lie on the dorsal surface of eIF4E relative to the cap-binding slot. Since the mouse eIF4E protein subjected to crystallographic analysis by Marcotrigiano *et al.* (1997) was an N-terminally truncated recombinant product (Δ27) there is some uncertainty about the positions of the N-terminal region with respect to the published structure. In particular, amino acids 37–39 (HPL) belong to an essential region of eIF4E (Vasilescu *et al.*, 1996) and are highly conserved, yet are not thought to be directly involved in cap binding (Marcotrigiano *et al.*, 1997; Matsuo *et al.*, 1997). The 37–39 motif lies close to two tryptophans (W43, W46) whose function is unclear. The data of Matsuo *et al.* (1997) on the yeast eIF4E–CHAPS micelle structure indicate that these are both surface residues, while mutational analysis of human eIF4E has implicated them in cap binding (Morino *et al.*, 1996).

Accordingly, we targeted the regions 37–39, 71–75 and 131–143 in a mutagenesis study intended to identify residues that are involved in the eIF4G-dependent modulation of eIF4E cap-binding affinity. L45 was also targeted for comparative purposes because it lies between the two tryptophans at positions 43 and 46, but is not likely to be a surface residue in yeast eIF4E. F74 was a further 'control' target because it is located at an inaccessible position near to W75. No other tryptophan residues were targeted because they had all been found previously to affect cap binding in yeast eIF4E (Altmann *et al.*, 1988). Mutagenesis of individual amino acids was performed in order to create derivatives of *S.cerevisiae* eIF4E with either conservative or non-conservative substitutions (Figure 4A). Two types of assay were used to assess the influence of these mutations on eIF4E–eIF4G binding: capture on a m^{7}GDP–Sepharose affinity material; and surface plasmon resonance (SPR) analysis. In the first of these, each recombinant mutant form of eIF4E was incubated with a molar equivalent amount of 4G-BD4E$_{His6}$ prior to binding on a m^{7}GDP–Sepharose affinity column (Figure 4B). Elution with m^{7}GDP revealed how much of the 4G-BD4E$_{His6}$ remained bound to eIF4E. Mutations at HPL37–39, W75, E72, V71 and G139 all reduced the proportion of 4G-BD4E$_{His6}$ bound to eIF4E on the column. Moreover, as would be expected in terms of the respective abilities of the substituted side chains to mimic their wild-type counterparts, less conservative mutations generally affected the interaction more markedly, at least at 4°C. It is also notable that a major change in F74, which is not expected to be a surface residue, had no effect on the binding behaviour of eIF4E. Mutation of one other residue that lies outside the identified regions and is probably not solvent exposed (L45) also had a relatively small effect on protein ligand binding. However, since L45A also showed reduced cap binding, this mutant may have a more general destabilizing effect on the conformation of eIF4E.

An important feature of these experiments was the observation that the eIF4E mutations with lower affinities for 4G-BD4E$_{His6}$ also showed reduced binding to the cap column. Since in the absence of 4G-BD4E$_{His6}$ all the isolated eIF4E mutant proteins except P38A, L45A and G139D bound the cap with the same low affinity typical of wild-type non-eIF4G-associated eIF4E (otherwise referred to as apo-eIF4E; data not shown), it is evident that highly localized structural changes that affect eIF4E–eIF4G binding also influence eIF4E–cap binding affinity by virtue of their ability to reduce the influence of eIF4G binding on the conformation of eIF4E.

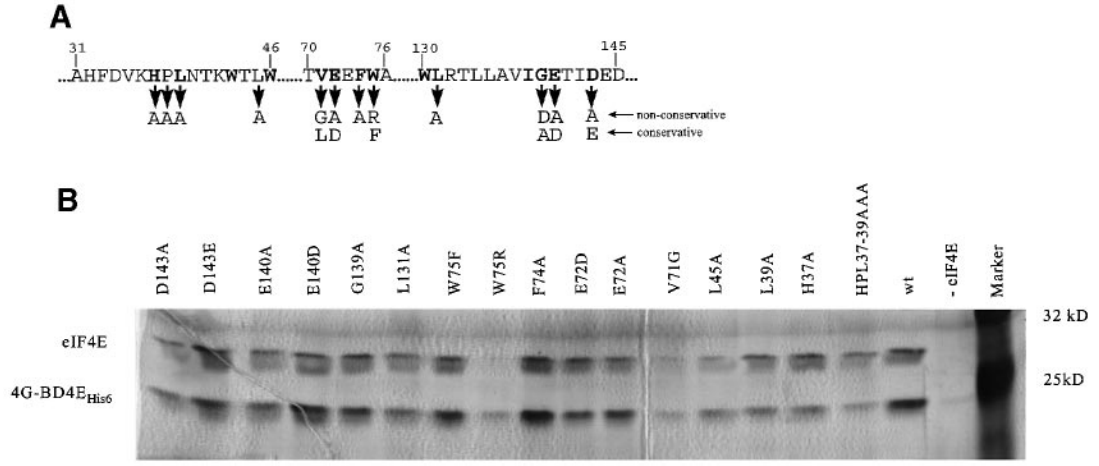

Fig. 4. Mutational analysis of surface residues on *S.cerevisiae* eIF4E. (**A**) A series of point mutations were generated via PCR in the eIF4E sequence. The amino acids printed in bold are absolutely conserved in all nine reported eIF4E sequences. P38 and L45 are conserved in all eIF4E sequences except that of wheat germ. All mutated residues except L39, L45 and F74 are predicted to be surface accessible on the basis of the mouse (Δ27) eIF4E crystal structure (Marcotrigiano *et al.*, 1997). (**B**) Each of the recombinant mutant proteins was generated in *E.coli* and used in binding experiments. After preincubation with recombinant 4G-BD4E$_{His6}$, the mixture was passed over m^{7}GDP–Sepharose, the cap-analogue-associated proteins subsequently being eluted using m^{7}GDP. In the control experiment (–eIF4E) eIF4E was omitted. These experiments were performed at 4°C.

More precise binding data were obtained using SPR analysis (Figure 5). 4G-BD4E$_{His6}$ was coupled to nickel-coated sensor chips and allowed to bind to the respective mutant forms of eIF4E (Figure 5A). The results revealed how the on- and off-rates for eIF4E binding were affected by the mutations, allowing the estimation of dissociation constants (Table I). Again, only a subset of the amino acid positions investigated seemed to be involved in complex formation. The relative 4G-BD4E$_{His6}$-binding affinity for wild-type eIF4E (K_d = 10^{-8}–10^{-9} l/mol) could be reduced at least 10-fold by single-site substitutions. Some apparent discrepancies between the changes in eIF4E–4G-BD4E$_{His6}$ binding affinity estimated using SPR as opposed to m^{7}GDP–Sepharose chromatography (Table I) turned out to be attributable to temperature-sensitive phenotypes.

The binding behaviour of two of the eIF4E mutations showed marked sensitivity to changes in ambient temperature. The more conservative substitutions at positions 72 (E72D) and 139 (G139A) showed relatively small reductions in 4G-BD4E$_{His6}$-binding at 4°C, while both resulted in strongly negative binding and growth phenotypes at higher temperatures (Table I). Thus, 4G-BD4E$_{His6}$ binding experiments performed at 25°C using SPR analysis (Table I) or at 20°C using m^{7}GDP–Sepharose chromatography (Figure 6A) revealed drastically attenuated binding at the higher temperature. This correlated with temperature sensitivity in the growth of strains dependent on these eIF4E mutant proteins (Table I). In control experiments (data not shown), the E72D form of eIF4E was found to bind m^{7}GDP–Sepharose in the absence of 4G-BD4E$_{His6}$ equally well at 4 and 25°C, the affinity observed being identical to that of wild-type eIF4E. This confirmed that the effect of the E72D mutation on eIF4E function was coupled to its influence on eIF4G binding, and not to any change in cap affinity caused directly by intramolecular structural alterations. The G139A mutation, in contrast, did show temperature sensitivity with respect to cap-binding. Therefore, both mutations at position 139 influence cap affinity and eIF4G binding directly.

p20–eIF4E binding involves a partially shared binding site

Since at the outset of this work p20 was suspected to be a negative regulator of eIF4E–eIF4G interactions *in vivo*, we examined the effects of the eIF4E mutations on eIF4E–p20 binding (see examples in Figure 5B). It was found that a more restricted set of the eIF4E mutations affected the binding constants calculated by means of SPR analysis (Figure 5B; Table I). Comparison of the binding data for 4G-BD4E$_{His6}$ and p20$_{His6}$ in Table I reveals that the mutants W75R and V71G showed reductions in binding affinity for both p20$_{His6}$ and 4G-BD4E$_{His6}$. In contrast, the mutations HPL37–39AAA, E72D, E72A and G139A reduced eIF4E–4G-BD4E$_{His6}$ binding to various degrees but had little or no effect on eIF4E–p20 binding. This means that the eIF4E binding sites for p20 and the eIF4G binding domain are not identical, but rather constitute overlapping sites that share a core set of amino acids.

Disruption of eIF4E–eIF4G binding inhibits translational initiation

We next examined at which point the eIF4E mutations disrupt translation and growth in yeast cells. The starting point for this part of the work was a diploid strain heterozygous for a disrupted *CDC33* gene, which upon sporulation can produce only two viable spores (GEX1; Vasilescu *et al.*, 1996). Upon transformation of this strain with a centromeric plasmid encoding eIF4E, sporulation can yield more than two viable spores if the plasmid-encoded eIF4E product is functional. Tetrad analysis was therefore performed on GEX1 transformants bearing the respective *CDC33* mutant genes expressed from the YCpSUPEX1 vector carrying the galactose-inducible P$_{GPF}$ promoter (Oliveira *et al.*, 1993). Sporulation was allowed to occur under conditions that allowed either full induction of the P$_{GPF}$ promoter (galactose medium), or only partial induction (galactose/glucose medium) which gave expression levels closer to those supported by the wild-type *CDC33* promoter. Analysis of those spores carrying the expression plasmid but no chromosomal *CDC33* gene

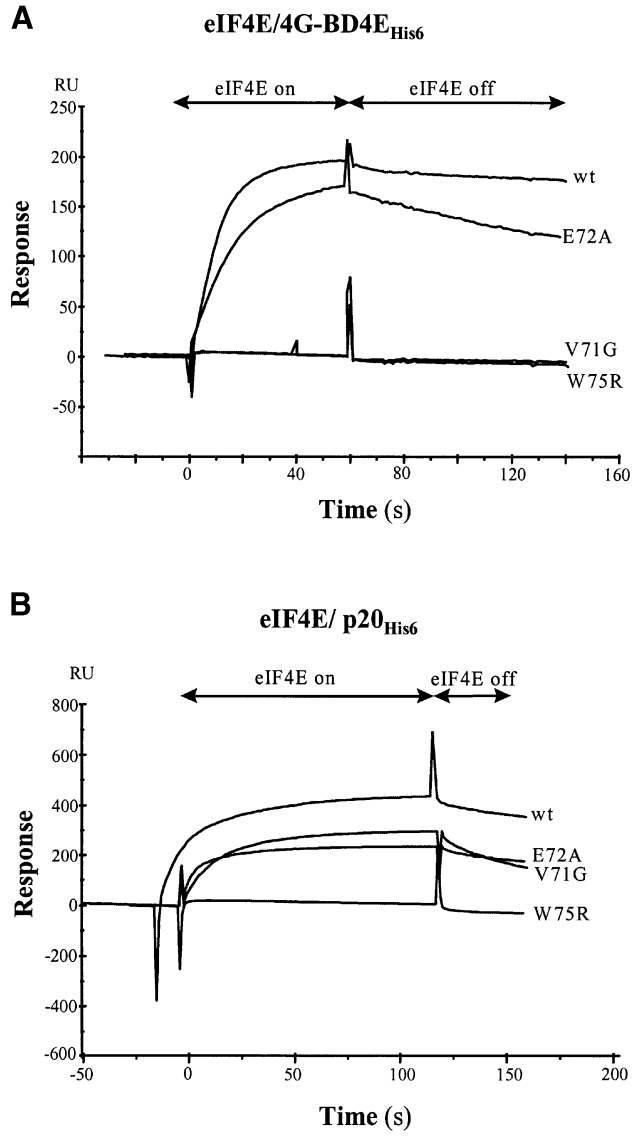

Fig. 5. SPR analysis of eIF4E interactions with 4G-BD4E$_{His6}$ and p20. The plots show how the SPR signal responded to the addition of eIF4E (at time 0) to a nickel-coated chip bearing either 4G-BD4E$_{His6}$ (**A**) or p20$_{His6}$ (**B**). Arrows above the traces indicate the phases of binding (after eIF4E addition) and of release (after exposure of the chip to eIF4E-free buffer). The results obtained with four different forms of eIF4E are shown. The estimated on- and off-rates calculated from experiments with the whole set of eIF4E proteins are summarized in Table I.

revealed a strict correlation between the ability of a point mutation to disrupt eIF4E–4G-4EBD$_{His6}$ binding *in vitro* and its ability to reduce cell viability. The complementation results shown in Table I derive from tetrad analyses performed on plates containing galactose/glucose medium at 30°C, which allowed expression of the *cdc33* mutant genes at a level comparable with that of the chromosomal wild-type gene (compare with Vasilescu *et al.*, 1996). All of the mutant haploid strains were found to be viable at 15 or 30°C upon overexpression of the respective *cdc33* mutant genes via full induction of the P_{GPF} promoter in galactose medium. In contrast, at 37°C two strains (carrying the mutations E72D and G139A) conferred inviability in galactose medium.

Polysomal gradient analysis of yeast cell extracts derived from one of the temperature-sensitive mutant strains revealed a shift in the distribution of ribosomal subunits to smaller polysomes and larger pools of non-translating monosome particles. For example, this effect is evident in a strain bearing the mutation E72D, which results in temperature-sensitive eIF4E–eIF4G binding (Figure 6). This is indicative of a block in the initiation phase of translation, as would be expected of defects that interfere with the mediation of the initial interactions between 40S ribosomal subunits and mRNA by the eIF4F complex. A further phenomenon typical of such an initiation defect is the appearance of a large population of non-translating 80S couples (Zhong and Arndt, 1993; Vasilescu *et al.*, 1996). Since these inactive 80S particles can be readily dissociated by high levels of salt, we examined the effect of including 0.8 M NaCl in the sucrose gradient (Figure 6F). The observed result confirmed that such inactive couples constitute a major proportion of the ribosome population in the mutant cells at the non-permissive temperature.

Discussion

A specific eIF4G binding site on eIF4E

The combination of *in vitro* and *in vivo* data presented in this work demonstrates that eIF4G modulates eIF4E–cap binding via its interaction with specific residues on the surface of eIF4E. The results of m^{7}GDP–Sepharose chromatography and SPR analyses provide generally consistent indications of the effects of the mutations on eIF4E interactions. However, while the cap-analogue affinity method can only give approximate indications of changes in eIF4E interactions with other proteins, the SPR procedure provides estimates of both on- and off-rates, and thus a much more accurate quantitative impression of how site-specific alterations affect protein binding (Table I). Overall, this combined experimental approach has generated a more complete picture of the biochemical consequences of the mutations, highlighting the large changes in binding affinity caused by even conservative alterations at certain sites. The SPR analysis has revealed that the eIF4E–4G-BD4E$_{His6}$ interaction is strong (K_d = 10^{-8}–10^{-9} l/mol) in comparison with the previously estimated affinity of non-complexed human eIF4E for the 5′ cap (K_d = 10^{-5}–10^{-7} l/mol, depending on the RNA ligand; Carberry *et al.*, 1989; Ueda *et al.*, 1991). However, we would estimate from our m^{7}GDP–Sepharose chromatography data that the yeast eIF4E–cap affinity is increased at least 10-fold upon interaction with 4G-BD4E$_{His6}$ (giving a $K_d \leqslant 10^{-7}$). A similar estimate of the magnitude of the cooperativity effect has been made on the basis of cross-linking results obtained with the mammalian eIF4F complex (Edery *et al.*, 1987; Haghighat and Sonenberg, 1997). Significantly, our experiments show that the marked increase in cap-binding affinity in the yeast system is induced by the association of eIF4E with the eIF4E-binding domain of eIF4G alone. Thus the other domains of eIF4G, including its RNA-binding motifs, are not required for the eIF4E–cap interaction to be stabilized. We conclude that the interaction between eIF4G and its binding site on eIF4E suffice to induce enhanced cap-binding, and no other interactions between eIF4G and the mRNA are likely to be required to stabilize eIF4F association with the 5′ end of the

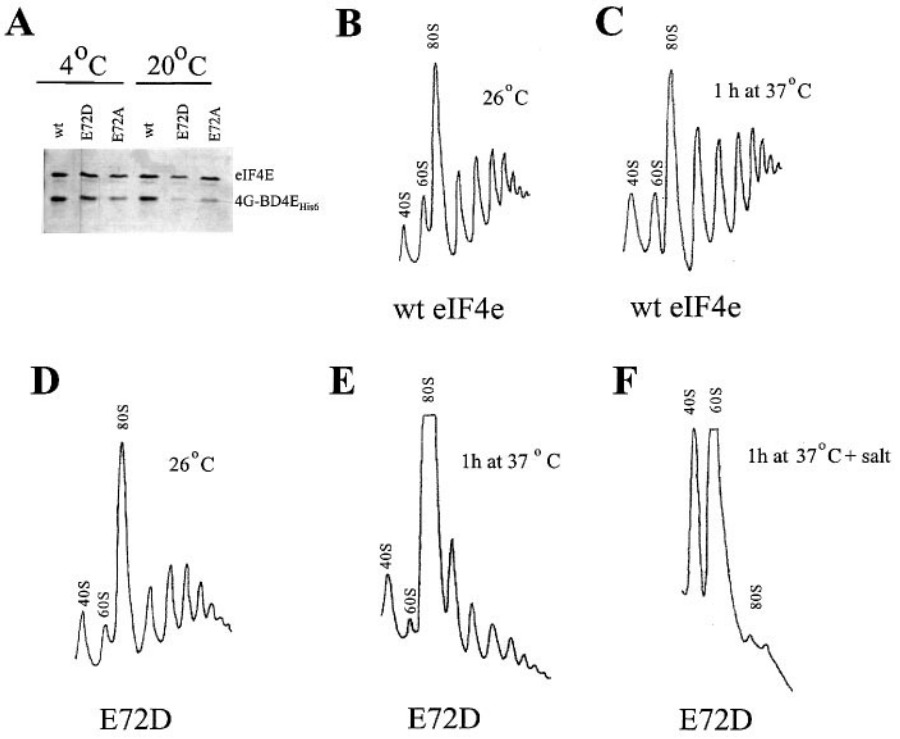

Fig. 6. A defective eIF4G-binding site on eIF4E prevents normal translational initiation. (**A**) Cap-analogue-chromatography revealed that, at 4°C, the less conservative mutation (E72A) bound 4G-BD4E$_{His6}$ less well than E72D. The conservative mutation (E72D), on the other hand, resulted in a temperature-sensitive binding phenotype, so that binding became very weak at 20°C. This was found to have drastic consequences for translation *in vivo*, as manifested by the polysome profiles distinguishable upon sucrose gradient analysis (compare **D**–**F** with **B** and **C**). Raising the growth temperature of E72D-containing cells from 26 to 37°C resulted in a reduction in the average size of polysomes and a shift to monosomes (compare D and E). Inclusion of salt in the sucrose gradient resulted in the dissociation of most of the 80S particles in the mutant at 37°C into 40S and 60S subunits, demonstrating that much of the 80S population comprised non-translating 40S–60S couples.

Table I. Properties of mutant forms of eIF4E

Mutation	Complementation of *cdc33::LEU2*	Growth in gal medium at			Binding to eIF4E		
	phenotype in gal/glu medium	15°C	30°C	37°C	eIF4G-BD4E$_{His6}$		p20$_{His6}$
	(30°C)				4°C (m^7GDP–Sepharose)[a]	25°C [SPR(K_d)]	25°C [SPR(K_d)]
wt	yes	+	+	+	++++	10^{-9}	10^{-8}
H37A	yes	+	+	+	++	n.d.	n.d.
P38A	no	+	+	+	n.d.	n.d.	n.d.
L39A	yes	+	+	+	+++	n.d.	n.d.
HPL37–39AAA	no	+	+	+	+	–	10^{-8}
L45A	yes	+	+	+	++++	10^{-8}	10^{-8}
V71G	no	+	+	+	n.q.	–	10^{-7}
E72D	no	+	+	–	+++	10^{-7}	10^{-8}
E72A	no	+	+	+	++++	10^{-8}	10^{-8}
F74A	yes	+	+	+	++++	10^{-9}	10^{-8}
W75F	yes	+	+	+	++++	10^{-9}	10^{-8}
W75R	no	+	+	+	n.q.	–	–
L131A	yes	+	+	+	++++	10^{-9}	10^{-8}
G139A	no	+	+	–	++++	–	10^{-8}
G139D	no	+	+	+	n.d.	n.d.	n.d.
E140D	yes	+	+	+	++++	10^{-9}	10^{-8}
E140A	yes	+	+	+	++++	10^{-9}	10^{-8}
D143E	yes	+	+	+	++++	10^{-9}	10^{-8}
D143A	yes	+	+	+	++++	10^{-9}	10^{-8}

[a]In this column: +, 0–25%; ++, 25–50%; +++, 50–75%; ++++, 75–100%. (Values are percent of binding to wild-type eIF4E.)
n.d., not determined.
n.q., no quantification possible.
–, no binding detected.

mRNA. Mutant forms of yeast eIF4E with reduced cap affinities have already been shown to support only attenuated rates of translational initiation in yeast (Vasilescu *et al.*, 1996), thus showing how critical the normal affinity is for optimal translation.

The eIF4E–4G-BD4E$_{His6}$ binding affinity we have estimated ($K_d = 10^{-8}$–10^{-9} l/mol) can be usefully compared with the binding affinities of other RNA- and DNA-binding proteins. It is higher than the estimated affinity between the monomers of the bacteriophage λ *cI* repressor ($K_d \geqslant 10^{-8}$ l/mol), and lower than the affinity of the λ repressor for its DNA operator elements ($K_d = \sim 10^{-10}$; Ptashne, 1967). Interestingly, even the enhanced binding affinity of eIF4E for the cap is much lower than the binding affinity of the λ repressor for its DNA target, and of the mammalian iron regulatory protein (IRP; $K_d = 10^{-8}$–10^{-11}, depending on the state of IRP; Haile *et al.*, 1989), which is an RNA-binding repressor. This probably reflects the requirement for eIF4E to cycle through a preinitiation complex, rather than to act as a repressor that blocks a processive reaction (see McCarthy and Kollmus, 1995).

We have characterized two new classes of point mutations on eIF4E. One type of mutation reduces eIF4E binding to the respective binding sites on both eIF4G and p20; the other affects exclusively, or primarily, binding to the eIF4G site (Figure 7). We have defined key residues involved in the eIF4G binding site on eIF4E, showing that their substitution by other amino acids interferes with the site's function as a docking point for eIF4G. The mapping performed using monoclonal antibodies and mutagenesis indicates that the residues 71–75 and 139 of yeast eIF4E are on the surface of the protein. They correspond to two regions of highly conserved amino acids predicted to be adjacent on the convex surface of mouse eIF4E that lies on the other side of the molecule from the cap-binding slot (Marcotrigiano *et al.*, 1997; Figure 7). Given the possible distortion of the mouse eIF4E crystal structure by the deletion of this protein's first 27 amino acids, the crystallographic data may not have provided a reliable indication of the position of residues 37–39 relative to the surface of wild-type eIF4E. However, both the crystal structure and the NMR structural data (Matsuo *et al.*, 1997) suggest that at least one of these residues is on the surface (as indicated in our representations of the published yeast structure in Figure 7). Our data indicate that this region is involved in eIF4G binding, and is indeed likely to be at least partially on the surface of wild-type yeast eIF4E. It should be emphasized that the majority of our mutations do not cause general destabilization of the conformation of the eIF4E molecule. This is evident from the observation that they influence localized interactions with 4G-BD4E$_{His6}$ without disturbing the binding behaviour of apo-eIF4E.

Our biochemical and genetic analyses of the surface mutations reveal that the efficiency of translational initiation and cell viability are closely tied to the affinity between eIF4E and eIF4G. This is underlined by the observation that a conservative mutation of a surface residue that is involved in eIF4G–eIF4E binding can disrupt normal ribosome–mRNA interactions. The relatively tight interaction between eIF4G and eIF4E is evidently important for the binding of 40S ribosomal subunits to mRNA, and a reduction in binding affinity of

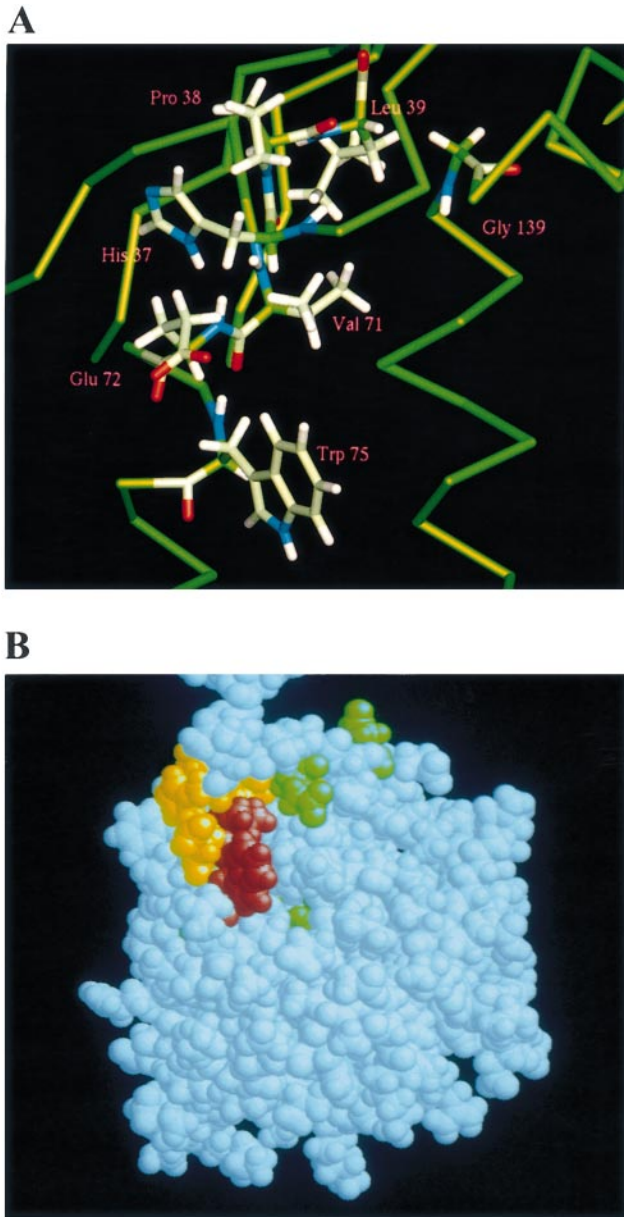

Fig. 7. Amino acids involved in eIF4G and p20 binding map to a predicted surface-accessible cluster on the dorsal surface of *S.cerevisiae* eIF4E. Based on the crystal structure of the mouse (Δ27) eIF4E protein (Marcotrigiano *et al.*, 1997) and the NMR structure of yeast eIF4E (Matsuo *et al.*, 1997), these groups of residues are predicted to lie together on the opposite face of yeast eIF4E from the cap-binding slot. They belong to α-helices 1 and 2, respectively, or are associated with a beta strand (β1) that follows the variable N-terminal region of the eIF4E sequence. We have used the coordinates of the published NMR structure in this figure as the basis for modelling the positions of the various mutations. (**A**) The backbone model of the core region in which mutations influenced binding. The side chains of the mutated amino acids are shown. (**B**) The same region in the context of a space-filling model of the whole molecule. The view is of the dorsal face angled to show the site clearly. The structure of the N-terminal region of the protein is unclear and has been cut off at the top of this representation. The amino acids are coloured according to their apparent contributions to eIF4G and/or p20 binding. Red marks the positions of amino acids that affect the binding of both 4G-BD4E$_{His6}$ and p20$_{His6}$ (V71 and W75); yellow indicates the sites of amino acids influencing only 4G-BD4E$_{His6}$ binding (E72, H37, P38, L39, G139); green denotes amino acids whose mutation had no effect on binding to either ligand (L45, L131, E140, D143). L131 is partly buried (green, bottom-right of the cluster) and F74 is completely buried (below E72 and W75) in this view. D143 is the separate, green residue top-right of the cluster.

<10-fold already has serious consequences for translation and cell growth.

p20 binds to an overlapping site

A further conclusion from this study is that p20 binding to eIF4E involves some, but not all, of the surface residues bound by 4G-BD4E$_{His6}$. In this work, we have examined the binding of a p20 protein that comprises only the amino acid sequence naturally encoded by the wild-type *CAF20* gene fused to six additional histidine residues. Most significantly, p20 binding interactions are restricted to the amino acids lying in the 71–75 region, and do not require the highly conserved amino acids in the regions 37–39 and 139 (Figure 7). The binding affinity of p20 for eIF4E estimated by SPR is ~10-fold less than that of the binding domain from eIF4G. At the same time, the binding assay data indicate that p20 is less capable of modulating eIF4E–cap affinity.

Overall, we therefore propose that p20 competes with eIF4G-binding to eIF4E because it shares part of the binding site recognized by the eIF4E-binding domain of eIF4G (Figure 7). Moreover, while the exact identity of the interaction sites on eIF4E is not the primary concern of this study, it is probable that the amino acids highlighted in Figure 7 either directly influence, or contribute to, the eIF4E-binding surface for eIF4G and p20. Crystallographic analysis of the eIF4E–eIF4G and eIF4E–p20 complexes will be required in order for the exact geometries of these interactions to be determined.

eIF4E cycling and regulation

The results of this study provide insight into the control of eIF4E function by eIF4G and p20. The binding of p20 to eIF4E can inhibit eIF4G–eIF4E complex formation because it blocks access to part of the eIF4G binding site on the eIF4E surface. The enhancement of eIF4E–cap binding affinity induced by eIF4G binding is partially mimicked by p20. We propose that the interactions between eIF4G and the three identified regions of eIF4E cause a conformationally-induced improved fit for the cap structure in the cap-binding slot located on the other side of eIF4E (Figure 8A).

The operation of heterotropic cooperativity in eIF4E binding provides a basis for understanding the molecular details of eIF4E function and regulation. Stabilization of the eIF4E–cap interaction (to a $K_d \leqslant 10^{-7}$ l/mol) is presumably required so that eIF4E (as a component of eIF4F) can mediate the interactions of the 40S ribosomal subunit with the 5′ end of the mRNA in the cell. Cycling of eIF4E on and off the mRNA will be mediated by the interaction with eIF4G in eIF4F. A model can be envisaged in which disruption of the eIF4E–eIF4G complex leads to release of eIF4E from the mRNA, allowing it to recycle (Figure 8B). The actual mechanism of this release step has yet to be ascertained. The quantitative measurements of protein–protein interactions show us that a tightly bound eIF4E–eIF4G complex is likely to be the primary species interacting with capped mRNA. This pathway of interaction can be disrupted by p20 binding to eIF4E, since the resulting complex prevents mediation of 40S binding to the 5′ end via eIF4G. The weak enhancement of eIF4E cap-binding activity afforded by the association with p20 will allow the eIF4E–p20 complex to compete

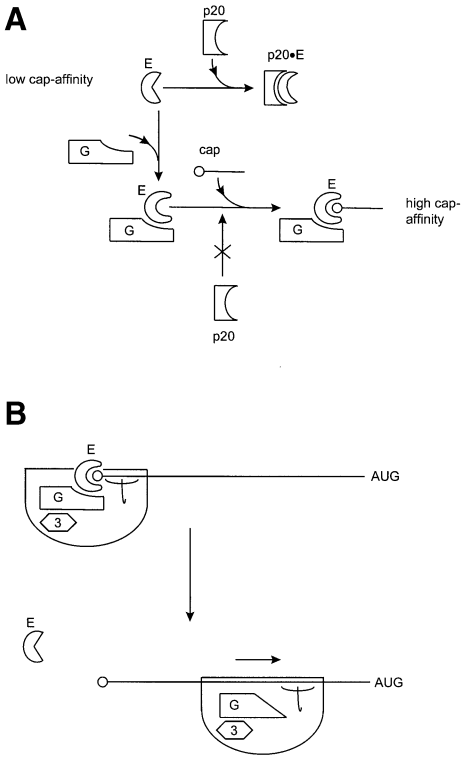

Fig. 8. Heterotropic cooperativity in eIF4E and the translational initiation cycle. (**A**) The association of eIF4E with eIF4G to form eIF4F induces a high-affinity cap-binding state in eIF4E. This promotes 40S–mRNA interactions and ultimately, translational initiation. p20 can bind to part of the eIF4G-binding site on eIF4E, generating potentially a dead-end complex unable to participate in the eIF4G-mediated initiation pathway. Since p20 binds with a lower affinity to eIF4E, it does not block translation, but rather exerts fine regulation via competition with eIF4G for a shared site on eIF4E. (**B**) The quantitative data presented in this paper provide the basis for understanding how a cyclical cap–eIF4E binding pathway might function. The balance of interactions between eIF4E and respectively eIF4G and p20 can be understood in terms of the relative affinities of these proteins. The binding of eIF4G mediates both enhanced cap-binding and association of the 40S ribosomal subunit. The relatively high affinity of eIF4G binding to eIF4E ensures that the latter binds to the 5′ cap almost exclusively as part of the eIF4F complex. Subsequently, and perhaps during scanning or as a result of 60S junction, a rearrangement of the preinitiation complex induces dissociation of eIF4E from eIF4G, which we have seen to cause loss of the high-affinity cap-binding state in eIF4E. As a result, eIF4E can be released relatively easily from the mRNA, thus becoming free to rebind eIF4G and thus restart another cycle.

effectively with apo-eIF4E, but less effectively with eIF4F, for binding to the 5′ cap of cellular mRNAs. However, the binding data also tell us that p20 is unable to compete very effectively with eIF4G for binding to eIF4E, thus explaining why the overexpression of *CAF20* has only a limited effect on cell growth (Lanker *et al.*, 1992; Altmann *et al.*, 1997; De la Cruz *et al.*, 1997). We therefore propose that p20 is likely to have evolved as part of a regulatory mechanism that fine-tunes translation. This explains why p20 is not essential for normal growth under standard laboratory conditions. Future studies of the physiological role of p20 will therefore need to focus on detailed analysis of the relationship between growth-limiting conditions and the mechanism modulating p20 activity.

Materials and methods

Monoclonal antibodies and epitope mapping

Lymphocytes from mice immunized with recombinant yeast eIF4E were fused with myeloma cells to obtain hybridoma cells (carried out by Eurogentec, Brussels). The resulting cell lines were plated out on 96-well plates in RPMI-HT medium supplemented with ultra low-IgG fetal calf serum (FCS; Gibco-BRL) to a density of ~1 cell/well and grown for 10–12 days. The culture supernatant was tested for antibodies in an ELISA-based assay with recombinant, native eIF4E immobilized on the plates. Wells with the strongest signals were plated out and tested in two further rounds of selection to ensure that the resulting antibodies were products of a single cell clone. For scaling up, cells from a 10 ml culture were transferred into 200 ml cultures and grown for 3–4 weeks. The antibodies were purified from the culture supernatant using agarose-coupled anti-mouse IgG (Sigma) according to the supplier's instructions. Yields varied between 2 and 25 mg antibody/1000 ml cell culture. Subtyping of the antibodies was performed using an ELISA-based isotyping kit (Sigma). The mapping of epitopes recognized by the respective monoclonal antibodies was performed using a library of membrane-bound peptides generated by means of spot-synthesis (Frank, 1992). The library comprised a series of overlapping dodecamer peptides representing the complete primary amino acid sequence of yeast eIF4E, each peptide being displaced by three amino acids relative to the preceding and following peptide. Selected antibodies were tested further on a membrane carrying a set of decamer peptides with a sequence displacement of only one amino acid. Prior to use, each peptide-loaded membrane was soaked with ethanol and Tris-buffered saline (TBS; 50 mM Tris pH 7.0, 150 mM NaCl) and then blocked in a solution of 1% gelatine in TBS (1 h at room temperature). Mouse monoclonal antibodies and secondary (goat anti-mouse) antibodies were applied in a solution of 0.2% gelatine in TBS, and the membrane then stained with MTT/BCIP in CBS (10 mM citric acid pH 7.0, 150 mM NaCl) until a clear signal was visible (maximum 20 min). Washes were performed with 0.5% Tween-20 (Sigma) in TBS. For each antibody the following cycle was performed: blocking, secondary antibody, staining (to ensure complete removal of antibodies from previous cycles); blocking, first antibody, secondary antibody, staining, stripping. For the stripping of old antibodies, the membrane was sonicated three times in denaturing buffer (8 M urea, 10% SDS, 0.5% β-mercaptoethanol, for 10 min at 40°C) and washed three times with wash buffer (50% ethanol, 10% acetic acid in H_2O) and twice with ethanol before it was dried and stored at –20°C.

Plasmid construction

Mutations of *S.cerevisiae CDC33* were prepared using the PCR method described by Mikaelian and Sergeant (1992). The PCR products were initially cloned in the TA-vector (Invitrogen). For expression of the mutant genes in *E.coli*, the fragments were subcloned as 0.6 kb pair *Nde*I–*Bam*HI fragments into the vector pCYTEXP1 (Belev *et al*., 1991). For expression in *S.cerevisiae*, the same fragments were subcloned into the single-copy vector YCpSUPEX cleaved with *Nde*I–*Bgl*II (Oliveira *et al*., 1993). Constructs for the production of *S.cerevisiae* p20 protein and the 4G-BD4E domain were provided with a His_6-tag via PCR amplification, and integrated into the expression vector as *Nde*I–*Eco*RI fragments.

Expression and genotype/phenotype analysis in S.cerevisiae

The diploid strain GEX1 (Vasilescu *et al*., 1996) was used for tetrad analysis after transformation using the lithium acetate method (Sherman *et al*., 1986). GEX1 was originally created by mating strains 4-2 {**a** *cdc33::LEU2 ura3 trp1 leu2* [pMDA101 *cdc33* (E73K, G179D)]; Altmann *et al.* (1989)} with SL988 (α *met8-1 leu2-1 his3Δ1 trp1 ura3-52*) and subsequent elimination of pMDA101 (Vasilescu *et al.*, 1996). Yeast cells were grown in rich medium (2% peptone, 1% yeast extract) containing either 0.5% galactose and 1.5% glucose for weak expression of mutant *S.cerevisiae cdc33* alleles or 2% galactose for strong expression. For the polysomal gradients we used complete medium containing 0.5% galactose and 1.5% glucose.

Sucrose density gradients

In a procedure adapted from Sagliocco *et al*. (1993), 50 ml yeast cultures of the strain containing either the wild-type *CDC33* gene or its mutant form E72D on the P_{GPF} expression vector YCpSUPEX1 were grown at 26°C in YEPD medium to an OD_{550} of 0.4. At this point the cultures were shifted to a 37°C water bath. Parallel cultures were maintained at 26°C. After 1 h, cycloheximide was added (50 μg/ml final concentration) and the cells were harvested for the preparation of extracts. The extracts were loaded onto 12 ml 15–40% sucrose gradients. Gradients were centrifuged for 2.5 h at 4°C and 39 000 r.p.m. in a Beckman SW40Ti rotor.

Synthesis and purification of recombinant proteins in E.coli

DNA cloning and sequencing techniques were performed using standard methods (Sambrook *et al*., 1989). The *E.coli* strains used for expression of the respective mutant forms of *cdc33* and of *caf20* and the *TIF4631* domain were TG2 [*supE hsdΔ5 thi Δ(lac-proAB) Δ(sre-recA) 306::Tn10 (tet^r) F′ (traD36pro AB$^+$ lacI^q lacZΔ M15)*] and CAG629 (Grossman *et al.*, 1984). The expressed proteins were purified on Ni-NTA–agarose (Qiagen) under denaturing conditions according to the supplier's protocols. Recombinant wild-type and mutant forms of eIF4E were purified as described previously (Edery *et al*., 1987; Lang *et al*., 1994).

Analytical m^{7}GDP-Sepharose chromatography

For analytical m^{7}GDP-chromatography 10–20 μg recombinant eIF4E were mixed with 40 μl m^{7}GDP–Sepharose (Pharmacia) and 4G-BD4E or p20 as stated in a total volume of 300 μl buffer A (20 mM HEPES pH 7.4, 100 KCl, 2 mM $MgCl_2$). The mixture was incubated on a shaker at 4°C for 2 h. The resin was then washed with 3× 1 ml of buffer A and bound proteins were eluted with 80 μl of 0.1 mM m^{7}GDP in buffer A. Aliquots (10–20 μl) of the eluted fraction were analysed on 12.5% SDS gels (Laemmli, 1970). For the assay determining the relative cap affinity of eIF4E in the presence or absence of 4G-BD4E and p20, 40 μl of m^{7}GDP–Sepharose were incubated with 15 μg recombinant eIF4E at 4°C for 20 min. The resin was washed once with 1 ml of buffer A and then incubated on a shaker for 2 h at 4 C in 1 ml buffer A containing 4G-BD4E or p20, respectively. Washing, elution and analysis were performed as above. The effects of monoclonal antibodies on the interaction between 4G-4EBD$_{His6}$ and eIF4E were assessed by adding 0.8 nmol of each antibody type to the protein mixture (0.2 nmol eIF4E + 0.2 nmol 4G-4EBD$_{His6}$) prior to addition to the cap-analogue matrix. Quantitative estimates of the relative effects on binding were made using image analysis software (Bio-Rad, UK) to compare the intensities of the silver-stained protein bands.

Surface plasmon resonance assays

All SPR assays were performed in a BIAcore 2000 (Biacore, UK). The Sensorchip NTA (Biacore) was used for immobilizing the His_6-tagged 4G-BD4E or p20, respectively, and wild-type and mutant forms of eIF4E were injected over the chip. Each cycle consisted of a 20 μl injection of 500 nM $NiCl_2$ in eluent buffer [10 mM HEPES pH 7.5, 100 mM KCl, 50 μM EDTA and 0.005% surfactant p20 (Biacore)], 50 μl of His-tagged protein in eluent buffer (resulting in ~250 RU of immobilized protein) and 40 μl of eIF4E in buffer A in a concentration range of 100–500 nM. The chip was regenerated after each cycle using 350 mM EDTA in eluent buffer. All measurements were performed at a flow rate of 20 μl/min at 25°C. The resulting sensorgrams were evaluated using the BIA Evaluation software package. The response from Ni-coated chips without immobilized protein was subtracted from the response obtained with 4G-BD4E- or p20-coated chips. The resulting curves were analysed using global fittings for Langmuir binding (4G-BD4E$_{His6}$) or Langmuir binding with drifting baseline (p20$_{His6}$). The values were checked for consistency using local fittings for each eIF4E concentration.

Molecular modelling

Three-dimensional representations of eIF4E and of the mutated sites on its surface were generated using RASMOL (Sayle and Milner-White, 1995) and Quanta 97 (v.97.0711 from Molecular Simulations Inc., Burlington, MA, USA) to process and display the coordinates provided by Matsuo and colleagues (Cambridge Protein Database).

Acknowledgements

We thank Heather Anderson and Sanj Kumar at Biacore UK for their support in setting up the SPR experiments, Andrea Tiepold (GBF) for expert assistance in the spot synthesis of peptides, and Dr Jeremy Derrick (UMIST, Department of Biomolecular Sciences) for help with the molecular modelling work. M.P. received support from the Biotechnology and Biological Sciences Research Council (BBSRC, UK), T.v.d.H. was supported by a Deutscher Akademischer Austauschdienst (DAAD) HSPIII stipend, S.V. was the recipient of a Royal Society/NATO Postdoctoral Fellowship Award and R.B. was supported by a Training Grant of the European Commission.

References

Altmann,M., Edery,I., Trachsel,H. and Sonenberg,N. (1988) Site-directed mutagenesis of the tryptophan residues in yeast eukaryotic initiation factor 4E. *J. Biol. Chem.*, **263**, 17229–17323.

Altmann,M., Müller,P.P., Pelletier,J., Sonenberg,N. and Trachsel,H. (1989) A mammalian translation initiation factor can substitute for its yeast homologue *in vivo*. *J. Biol. Chem.*, **264**, 12145–12147.

Altmann,M., Schmitz,N., Berset,C. and Trachsel,H. (1997) A novel inhibitor of cap-dependent translation initiation in yeast: p20 competes with eIF4G for binding to eIF4E. *EMBO J.*, **16**, 1114–1121.

Belev,T.N., Singh,M. and McCarthy,J.E.G. (1991) A fully modular vector system for the optimisation of gene expression in *Escherichia coli*. *Plasmid*, **26**, 147–150.

Browning,K.S. (1996) The plant translational apparatus. *Plant Mol. Biol.*, **32**, 107–144.

Carberry,S.E., Rhoads,R.E. and Goss,D.J. (1989) A spectroscopic study of the binding of m^7GTP and m^7GpppG to human protein-synthesis initiation factor-4E. *Biochemistry*, **28**, 8078–8083.

Craig,A.W.B., Haghighat,A., Yu,A.T.K. and Sonenberg,N. (1998) Interaction of polyadenylate-binding protein with the eIF4G homologue PAIP enhances translation. *Nature*, **392**, 520–523.

De la Cruz,J., Iost,I., Kressler,D. and Linder,P. **(**1997) The p20 and DED1 proteins have antagonistic roles in eIF4E-dependent translation in *Saccharomyces cerevisiae*. *Proc. Natl Acad. Sci. USA*, **94**, 5201–5206.

Edery,I., Lee,K.A.W. and Sonenberg,N. (1987) In Illan,I. (ed.), *Translational Regulation of Gene Expression*. Plenum Press, New York, NY, pp. 335–366.

Frank,R. (1992) Spot-synthesis: an easy technique for the positionally addressable, parallel chemical synthesis on a membrane support. *Tetrahedron*, **48**, 9217–9232.

Goyer,C., Altmann,M., Lee,H.S., Blanc,A., Deshmukh,M., Woolford,J.L., Trachsel,H. and Sonenberg,N. (1993) *TIF4631* and *TIF4632*: two yeast genes encoding the high-molecular-weight subunits of the cap-binding protein complex (eukaryotic initiation factor 4F) contain an RNA recognition motif-like sequence and carry out an essential function. *Mol. Cell. Biol.*, **13**, 4860–4874.

Gradi,A., Imataka,H., Svitkin,Y.V., Rom,E., Raught,B., Morino,S. and Sonenberg,N. (1998) A novel functional human eukaryotic translation initiation factor 4G. *Mol. Cell. Biol.*, **18**, 334–342.

Grossman,A.D., Erickson,J.W. and Gross,C.A. (1984) The *htpR* gene product of *E.coli* is a sigma factor for heat-shock promoters. *Cell*, **38**, 383–390.

Haghighat,A. and Sonenberg,N. (1997) eIF4G dramatically enhances the binding of eIF4E to the mRNA 5′-cap structure. *J. Biol. Chem.*, **272**, 21677–21680.

Haile,D.J., Hentze,M.W., Roualt,T.A., Harford,J.B. and Klausner,R.D. (1989) Regulation of interaction of the iron-responsive element binding-protein with iron-responsive RNA elements. *Mol. Cell. Biol.*, **9**, 5055–5061.

Harlow,E. and Lane,D. (1988) *Antibodies: A Laboratory Manual*. Cold Spring Harbor Laboratory Press, Cold Spring Harbor, NY.

Laemmli,E.K. (1970) Cleavage of structural proteins during the assembly of the head of bacteriophage T4. *Nature*, **227**, 680–685.

Lamphear,B.J., Kirchweger,R., Skern,T. and Rhoads,R.E. (1995) Mapping of functional domains in eukaryotic protein synthesis initiation factor 4G (eIF4G) with picornaviral proteases. *J. Biol. Chem.*, **270**, 21975–21983.

Lang,V., Zanchin,N., Lünsdorf,H., Tuite,M.F. and McCarthy,J.E.G. (1994) Initiation factor eIF-4E of *Saccharomyces cerevisiae*: distribution within the cell, binding to mRNA and consequences of its overproduction. *J. Biol. Chem.*, **269**, 6117–6123.

Lanker,S., Müller,P.P., Altmann,M., Goyer,C., Sonenberg,N. and Trachsel,H. (1992) Interactions of the eIF-4F subunits in the yeast *Saccharomyces cerevisiae*. *J. Biol. Chem.*, **267**, 21167–21171.

Le,H., Tanguay,R.L., Balasta,M.L., Wei,C.-C., Browning,K.S., Metz,A.M., Goss,D.J. and Gallie,D.R. (1997) Translation initiation factors eIF-iso4G and eIF-4B interact with the poly(A)-binding protein and increase its RNA binding activity. *J. Biol. Chem.*, **272**, 16247–16255.

Mader,S., Lee,H., Pause,A. and Sonenberg,N. (1995) The translation of initiation factor eIF-4E binds to a common motif shared by the translation factor eIF-4γ and the translational repressors 4E-binding proteins. *Mol. Cell. Biol.*, **15**, 4990–4997.

Marcotrigiano,J., Gingras,A.-C., Sonenberg,N. and Burley,S.K. (1997) Cocrystal structure of the messenger RNA 5′ cap-binding protein (eIF4E) bound to 7-methyl-GDP. *Cell*, **89**, 951–961.

Matsuo,H., Li,H., McGuire,A.M., Fletcher,C.M., Gingras,A.-C., Sonenberg,N. and Wagner,G. (1997) Structure of translation factor eIF4E bound to m^7GDP and interaction with 4E-binding protein. *Nature Struct. Biol.*, **4**, 717–724.

McCarthy,J.E.G. (1998) Posttranscriptional control of gene expression in yeast. *Microbiol. Mol. Biol. Rev.*, in press.

McCarthy,J.E.G. and Kollmus,H. (1995) Cytoplasmic mRNA-protein interactions in eukaryotic gene expression. *Trends Biochem. Sci.*, **20**, 191–197.

Merrick,W.C. and Hershey,J.W.B. (1996) The pathway and mechanism of eukaryotic protein synthesis. In Hershey,J.W.B., Matthews,M.B. and Sonenberg,N. (eds), *Translational Control*. Cold Spring Harbor Laboratory Press, Cold Spring Harbor, NY, pp. 31–70.

Mikaelian,I. and Sergeant,A. (1992) A general and fast method to generate multiple site directed mutations. *Nucleic Acids Res.*, **20**, 376.

Morino,S., Hazama,H., Ozaki,M., Teraoka,Y., Shibata,S., Doi,M., Ueda,H., Ishida,T. and Uesugi,S. (1996) Analysis of the mRNA cap-binding ability of human eukaryotic initiation factor-4E by use of recombinant wild-type and mutant forms. *Eur. J. Biochem.*, **238**, 597–601.

Morley,S.J., Curtis,P.S. and Pain,V.M. (1997) eIF4G: Translation's mystery factor begins to yield its secrets. *RNA*, **3**, 1085–1104.

Oliveira,C.C., van den Heuvel,J.J. and McCarthy,J.E.G. (1993) Inhibition of translational initiation in *Saccharomyces cerevisiae* by secondary structure: the role of the stability and position of stem-loops in the mRNA leader. *Mol. Microbiol.*, **9**, 521–532.

Pause,A., Belsham,G.J., Gingras,A.-C., Donzé,O., Lin,T.-A., Lawrence,J.C.,Jr and Sonenberg,N. (1994) Insulin-dependent stimulation of protein synthesis by phosphorylation of a regulator of 5′-cap function. *Nature*, **371**, 762–767.

Ptashne,M. (1967) Specific binding of the λ phage repressor to λ DNA. *Nature*, **214**, 232–234.

Ptushkina,M., Fierro-Monti,I., van den Heuvel,J., Vasilescu,S., Birkenhäger,R., Mita,K. and McCarthy,J.E.G. (1996) *Schizosaccharomyces pombe* has a novel eukaryotic initiation factor 4F complex containing a cap-binding protein with the human eIF4E C-terminal motif KSGST. *J. Biol. Chem.*, **271**, 32818–32824.

Rozen,F., Edery,I., Meerovitch,K., Dever,T.E., Merrick,W.C. and Sonenberg,N. (1990) Bidirectional RNA helicase activity of eucaryotic translation initiation factors 4A and 4F. *Mol. Cell. Biol.*, **10**, 1134–1144.

Sagliocco,F., Vega Laso,M.R., Zhu,D., Tuite,M.F., McCarthy,J.E.G. and Brown,A.J.P. (1993) The influence of 5′ secondary structures upon ribosome binding to mRNA during translation in yeast. *J. Biol. Chem.*, **268**, 26522–26530.

Sambrook,J., Fritsch,E.F. and Maniatis,T. (1989) *Molecular Cloning: A Laboratory Manual*. Cold Spring Harbor Laboratory Press, Cold Spring Harbor, NY.

Sayle,R.A. and Milner-White,E.J. (1995) RASMOL: biomolecular graphics for all. *Trends Biochem. Sci.*, **20**, 374–376.

Sherman,F., Fink,G.R. and Hicks,J.B. (1986) *Laboratory Course Manual for Methods in Yeast Genetics*. Cold Spring Harbor Laboratory Press, Cold Spring Harbor, NY.

Sonenberg,N. (1996) mRNA 5′ Cap-binding protein eIF4E and control of cell growth. In Hershey,J.W.B., Matthews,M.B. and Sonenberg,N. (eds), *Translational Control*, Cold Spring Harbour Laboratory Press, Cold Spring Harbour, NY, pp. 245–269.

Tarun,S.Z. and Sachs,A.B. (1996) Association of the yeast poly(A) tail binding protein with translation initiation factor eIF-4G. *EMBO J.*, **15**, 7168–7177.

Tarun,S.Z., Wells,S.E., Deardorff,J.A. and Sachs,A.B. (1997) Translation initiation factor eIF4G mediates *in vitro* poly(A) tail-dependent translation. *Proc. Natl Acad. Sci. USA*, **94**, 9045–9051.

Ueda,H., Maruyama,H., Doi,M., Inoue,M., Ishida,T., Morioka,H., Tanaka,T., Nishikawa,S. and Uesugi,E. (1991) Expression of a synthetic gene for human cap binding-protein (human IF-4E) in *Escherichia coli* and fluorescence studies on interaction with messenger-RNA cap structure analogs. *J. Biochem. (Tokyo)*, **109**, 882–889.

Vasilescu,S., Ptushkina,M., Linz,B., Müller,P.P. and McCarthy,J.E.G. (1996) Mutants of eukaryotic initiation factor eIF-4E with altered mRNA cap binding specificity reprogram mRNA selection by ribosomes in *Saccharomyces cerevisiae*. *J. Biol. Chem.*, **271**, 7030–7037.

Zanchin,N.I.T. and McCarthy,J.E.G. (1995) Characterization of the *in vivo* phosphorylation sites of the mRNA-cap-binding complex proteins eukaryotic initiation factor-4E and p20 in *Saccharomyces cerevisiae*. *J. Biol. Chem.*, **270**, 26505–26510.

Zhong,T. and Arndt,K.T. (1993) The yeast SIS1 protein, a DnaJ homolog, is required for the initiation of translation. *Cell*, **73**, 1175–1186.

Received April 14, 1998; revised May 26, 1998; accepted June 16, 1998